High quantum efficiency of 1.8?m luminescence in Tm3+fluoride tellurite glass

D Tang, Qingsong Liu, X Liu, Xu Wang, X Yang, Yongyan Liu, Tian Ying, Ye Renguang, Xianghua Zhang, Shiqing Xu

High quantum efficiency of 1.8 μm luminescence in Tm^{3+} fluoride tellurite glass

Dingchen Tang[a], Qingsong Liu[a], Xiujie Liu[a], Xu Wang[a], Xueying Yang[a], Yongyan Liu[a], Ying Tian[a,*], Renguang Ye [a,*], Xianghua Zhang[b], Shiqing Xu[a,*]

[a]*Key Laboratory of Rare Earth Optoelectronic Materials and Devices of Zhejiang Province, Institute of Optoelectronic Materials and Devices, China Jiliang University, Hangzhou 310018, People's Republic of China*

[b]*ISCR (Institut des Sciences Chimiques de Rennes) UMR 6226, Univ Rennes, CNRS, F35000, Rennes, France*

Abstract

In this paper, Tm^{3+} doped fluorotellurite glasses are synthesized by melt-quenching technique. The thermal and spectral properties of the glasses are characterized. The effect of the 1.8 μm emission properties for different Tm^{3+} concentrations are investigated. ΔT (153℃) of the glass indicates it has good thermal stability. Spectroscopic parameters of Tm^{3+} such as radiative transition probability, branching ratio, spectroscopic quality factor, integrated emission cross section and radiative lifetime are calculated on the basis of Judd-Ofelt analysis. The maximum half-height width corresponding to 1.8 μm broadens as Tm^{3+} increases and reaches a maximum of 216 nm, as well as the longer lifetime (5.68 ms). For 1.8μm ($^3F_4 \rightarrow {}^3H_6$) emission band, the calculated Tm^{3+} doped fluorotellurite glass has a high quantum efficiency of 75.93%. Furthermore, the theoretical analysis of the energy transfer mechanism between Tm^{3+} ions were represented. Therefore, these results demonstrate that prepared Tm^{3+} doped fluorotellurite glass is an ideal laser material for 1.8 μm band solid-state laser applications.

1. Introduction

In recent years, the development of 1.8 μm solid-state lasers have aroused great interests for potential applications, including laser ranging, air pollution monitoring, and eye safety laser surgery[1-4]. Due to their unique incomplete 4f electron layer, rare earth ions play an important role in the laser generation process. A number of experiments have proved that Tm^{3+}, Ho^{3+} perform well in luminescence of 1.8 μm because of the transition between energy levels Tm^{3+}: $^3F_4 \rightarrow {}^3H_6$ or Ho^{3+}: $^5I_7 \rightarrow {}^5I_8$[5-12]. However, Ho^{3+} cannot be directly pumped by available commercial 808 nm and 980 nm lasers diodes because it lacks a matching absorption band, while Tm^{3+} has a strong absorption band around 800 nm[13, 14]. It can be effectively pumped by commercial 808 nm lasers. In this article, Tm^{3+} doped glass was chosen as the candidate for 1.8 μm solid-state lasers.

The emissions efficiency of rare earth doped glass depends on the characteristics of the matrix glass. Therefore, a suitable host glass is also an important part of 1.8 μm luminescence. Most of the research has focused on tellurite glass[15, 16], silicate glass[17]and fluoride glass[18, 19]. In a variety of oxide glasses, tellurite glass is considered having low energy ($700cm^{-1}$), high refractive index and wide infrared transmittance range, but at the same time, it has some problems such as high thermal expansion coefficient and poor chemical stability. Silicate glasses have great physical chemical durability and thermal stability, but the high phonon energy of silicate glasses ($1100cm^{-1}$) limits development in Mid-infrared radiation(MIR) band[17, 20]. As we all know, lower phonon energy is beneficial for suppressing the probability of non-radiative transition. Fluoride glass has a lower phonon energy ($600cm^{-1}$)[21], which leads to a lower probability of non-radiative transition and improved MIR luminescence property. On the other hand, fluoride glass has high solubility of rare earth ions and excellent transmittance. However, the disadvantages of fluoride glass are poor mechanical properties and harsh preparation conditions. How to improve the physical and chemical properties of fluoride glass while ensuring the optical properties has always been the research focus of many researchers. With the introduction of TeO_2, the thermal stability and mechanical strength of the prepared fluorotellurite glass have been significantly improved[22]. Moreover, the laser and optical properties of fluorinated glass are greatly improved. So far, it has been reported that strong 1.8 μm fluorescence is obtained in tellurite and fluoride glasses[3, 18] , which leads to a lower probability of non-radiative transition and improved MIR luminescence property. On the other hand, fluoride glass has high solubility of rare earth ions and excellent transmittance. However, the disadvantages of fluoride glass are poor mechanical properties and harsh preparation conditions. How to improve the physical and chemical properties of fluoride glass while ensuring the optical properties has always been the research focus of many researchers. With the introduction of TeO_2, the thermal stability and mechanical strength of the prepared fluorotellurite glass have been significantly improved[22]. Moreover, the laser and optical properties of fluorinated glass are greatly improved. So far, it has been reported that strong 1.8 μm fluorescence is obtained in tellurite and fluoride glasses

2. Experimental

Tm^{3+} doped fluorotellurite glass with weight percentage composition of 85(AlF_3-MgF_2-CaF_2-SrF_2-BaF_2-YF_3)-15TeO_2-xTm_2O_3(where x = 0, 2.1, 2.8, 3.5, 4.2, named as AYT0 to AYT4). The reagents used in the experiment are all analytically pure (99.99% purity or higher). For each sample, the well-mixed analytic-grade raw materials (15g) with the required proportion were mixed and melted for 20min in an alumina crucible of 900°C under a normal atmosphere. Subsequently, the heated glass solution is poured into preheated mold and annealed for 2h at 420 ℃. Finally, the annealed glass sample was cut into 10mm×10mm×1mm and polished for testing.

The characteristic temperature (temperature of glass transition of T_g and temperature of initial crystallization of T_x) of the sample is determined by Netzschsta 449 /C differential scanning calorimetry (DSC) at a rate of 10K /min. The density of

AYT glass is measured by Archimedes method in distilled water. The Raman spectrum of the glass is measured with Renishaw in Via Raman microscope in the 400~1000 cm^{-1} spectrum range using a 532 nm excitation. Infrared transmittance was measured by Perkin-Elmer 1600 series infrared spectrometer. The absorption spectra of 400 nm~ 2200 nm are recorded on the Perkin-Elmer 900 UV/Vis/NIR spectrophotometer. The fluorescence spectra (1550~2150nm) are measured with a computer controlled Triax 320 type spectrometer and detected with a liquid-nitrogen-cooled PbS detector from 1550 to 2150 nm upon excitation by 808 nm LD. The decay curves are recorded with a digital phosphor oscilloscope (TDS3000C). The fluorescence lifetime of 1.8 μm is recorded by light pulses of the 808nm LD and HP546800B 100-MHz oscilloscope. All the measures are taken at room temperature and other conditions are kept as same as possible.

3. Results and discussion

3.1. Thermal properties

Figure 1 and the inset show different thermal scanning curves of the samples without any doping ions at a heating rate of 10 K/min. As we known, the values of the parameters T_g is an important factor for a laser glass, and the glass transition temperature (T_g) of prepared fluoride glass is 448℃, while the T_g of AYT glass can reach 534℃. It is obviously find that the introduction of TeO_2 will greatly improve the glass transition temperature. Compared with other T_g of fluoride glass[23] and tellurite glass[24], the AYT glass has a good thermal stability to resist thermal damage at high pumping power.

The ΔT (ΔT = (Tx -Tg)) is used to evaluate the glass stability or resistance to recrystallization during fiber drawing [25]. So it is expected that ΔT of glass is as large as possible to obtain a relatively wide range of temperature during fiber fabricating [26, 27] . In general, ΔT > 100℃ is beneficial for glass fiber drawing, since the fiber drawing is a re-heating process. The crystallization in the fiber drawing will increase the internal scatter losses and reduce the performance of the drawing optical fiber. After adding TeO_2, the characteristic temperature of fluorotellurite glass changes obviously. Compared with fluoride glass without TeO_2, the ΔT of fluorotellurite glass is large. The ΔT temperature of AYT glass reaches 153℃, which is much larger than prepared fluoride glass matrix (ΔT=120℃). In addition, it is obviously larger than the reported values for ZBLAN (ΔT=67.1℃) glass[28] and tellurite glasses[29]. The thermal stability and forming ability of glass have been significantly improved. It is inferred that the addition of TeO_2 will break the Te-O bond and form the Te-F bond. At the same time, free O^{2-} will join the network of the glass. Therefore, the improvement of the glass forming ability comes from the recombination of the structure. Excellent physicochemical properties of the prepared AYT glasses provide a powerful basis for their use in high-power applications of MIR lasers.

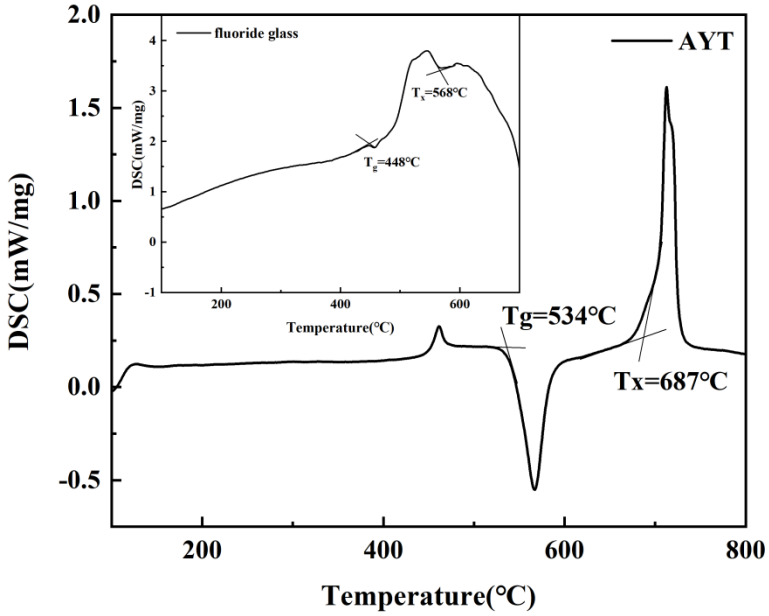

Fig.1 DSC curve of AYT glass host at the heating rate of 10 K/min. The inset is DSC curve of fluoride glass.

3.2.Infrared transmission spectrum

Figure 2 shows the infrared transmission spectrum of AYT glass. It is not difficult to find that AYT glass exhibits high transmittance in the range of 2000-4000 cm^{-1}. The transmittance can reach as high as 91% and 9% loss is caused by Fresnel reflection[30]. It is well known fact that the presence of OH^- content will affect the quantum efficiency of rare earth ions and optical losses, because OH^- will participate in the energy transfer between rare earth ions[31] . The content of OH^- groups in the glass can be expressed by the absorption coefficient of the OH^- vibration band at 3700 cm^{-1}, and given by the formula[22]:

$$\alpha[OH^-] = \frac{\ln(T_0/T)}{d} \quad (1)$$

where d is the thickness of the sample in millimeters, T_0 is the transmittance at the baseline, and T is the minimum transmittance near 3 μm. The hydroxyl content was calculated as 0.53 cm^{-1}, which is lower than that in bismuthate glass (0.71cm^{-1})[30]. The great infrared transmission property provides the fluorotellurite glass potential application for infrared laser materials.

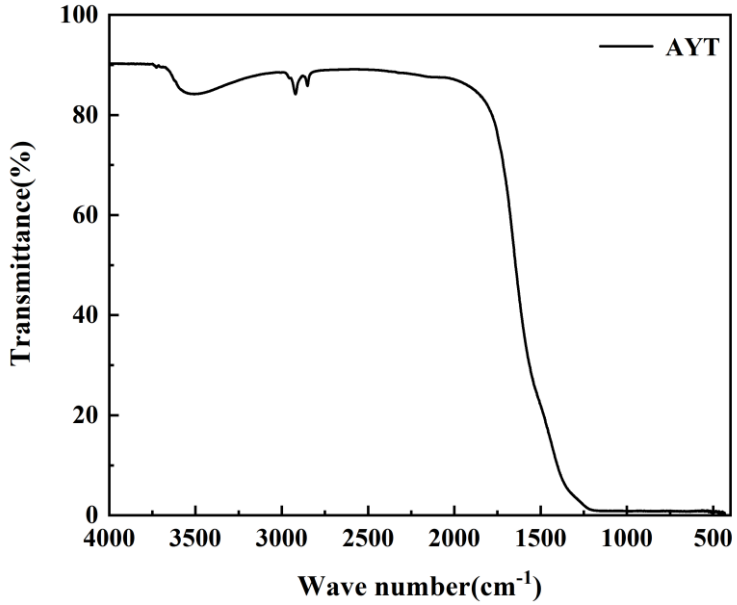

Fig.2 Infrared transmission spectrum of the AYT glass

3.3. Raman spectrum

For the sake of illustrating the effect of structure on 1.8 μm emission, Raman spectrum of AYT host glass in the range of 400 cm^{-1}-1000 cm^{-1} was measured and shown in Figure 3. Three peaks are obtained by Gaussian convolution fitting Raman spectrum, corresponding to 556 cm^{-1}, 749 cm^{-1} and 815 cm^{-1}, respectively. The Al-F bond vibration of [AlF_6] octahedral structural unit corresponds to the Raman absorption peak at 556cm^{-1}. At the same time, F^- ion in Al-F network is substituted to form [F_nAl-O-AlF_n unit and [Al-O-Al] structure. Nabazal[32] found that the Raman peak position of (TeO_3) unit appeared at 775cm^{-1} when fluoride was introduced into tellurite glass. In addition, the [TeO,F]$_4$ structural units in the fluorotellurite glass structure will lead to the Raman peak position of [TeO_3]unit moving to a high-frequency Raman band. In addition, with the introduction of TeO_2, the Raman spectrum of fluorotellurite glass appear a strong Raman peak at 815cm^{-1}, which was ascribed to the Te-O vibration in [TeO_4] groups. It is worth noting that the maximum phonon energy of AYT host glass is 815cm^{-1}, which is less than tellurite glass (832cm^{-1})[15] and silicate glass (970cm^{-1})[17].

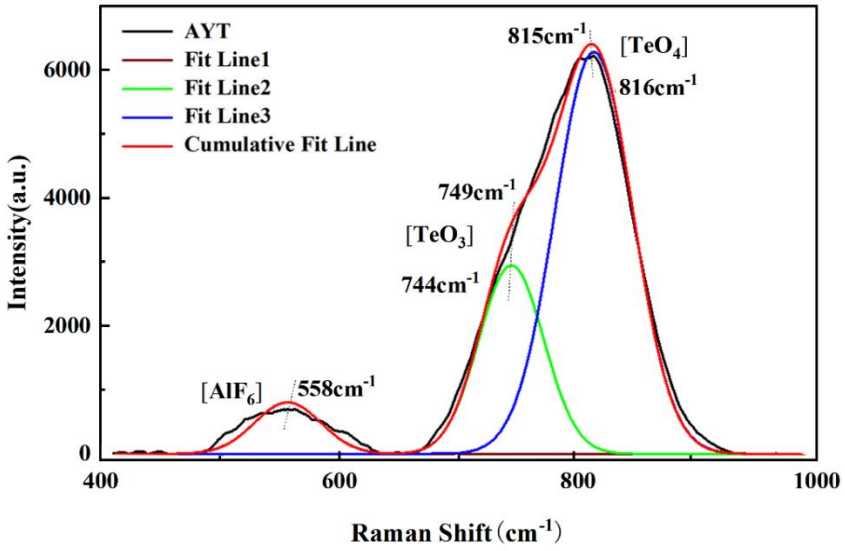

Fig.3 Raman spectra of AYT glass

3.4. Absorption spectra and J-O analysis

Figure 4 shows the optical absorption spectra of the Tm^{3+} doped samples in wavelength region of 400-2200 nm at room temperature. The five absorption bands of the spectra shown in the figure are 1673 nm, 1205 nm, 790 nm, 683 nm, and 468 nm, corresponding to the transitions from the ground state $^3H_6$ to the excited states $^3F_4$, $^3H_5$, $^3H_4$, $^3F_2$+$^3F_3$, and $^1G_4$, respectively. Owing to the intrinsic band gap absorption in the host glass, energy states higher than $^1D_2$ are not observed. There is no apparent change in the shape and position of each peak compared with other reported Tm^{3+} doped matrix glasses[33] . The results show that Tm^{3+} ions are homogeneously distributed in the present glassy network without obvious clusters. It is worth noting that a strong absorption band exists around 790 nm, which indicates it can be efficiently pumped with a commercial 808 nm laser diode.

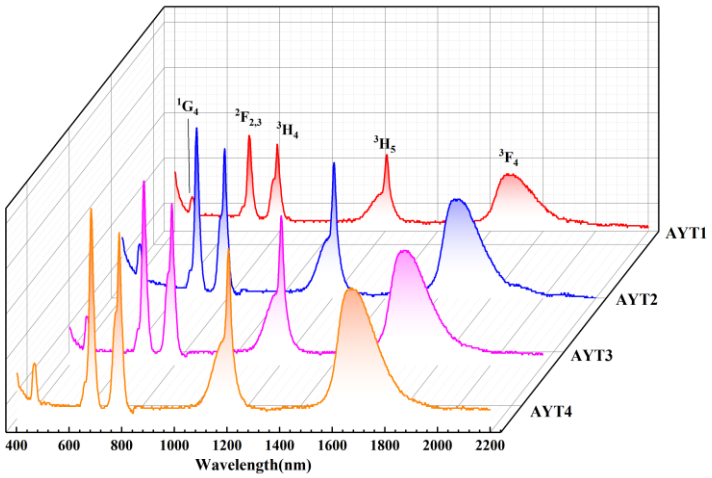

Fig.4 Absorption spectra of Tm^{3+} doped AYT glasses

To determine the transition probability of RE particles and the co-ordination structure, the luminescent intensity of RE ions can be calculated according to J-O theory in a certain range of accuracy, which is often used for evaluating the spectral properties of rare-earth doped glasses[33, 34] . J-O parameters are gained for further evaluation of the differences of ligand fields in different glasses. Then the J-O parameters of Tm^{3+} ion in present glass has been calculated by the least square fitting procedure. In general, Ω_2 provides information on the local environment of rare earth ions sites and the point symmetry of the environment around the Tm^{3+} ions. As seen in the Tablet 1, the Ω_2 of prepared glasses are larger than that of fluoride glass($1.14\times10^{-20}cm^2$), which is owing to the increase in ligand covalency from fluoride to oxide due to the lower polarizability of F^- than O^{2-}. The Ω_6 is related to overlapping integrals located in different 4f-5d orbitals in various matrix glasses and the value of Ω_6 gets bigger as the number of overlapping orbitals increases[5]. The Ω_6 of AYT3 glass is bigger than that of fluoride glass and tellurite glass as shown in Table 1. Therefore, J-O analysis shows that the prepared AYT3 glass has a stronger covalency and larger overlap integral.

Based on the J-O theory, the fluorescence spectra and strength parameter (Ω_t, t= 2, 4, 6) of fluorotellurite glasses can be used to calculate the spontaneous transition probability (A_{rad}), branching ratio (β), and theory lifetime (τ_{rad}), the results are shown in Table 2. It is worth to note that the spontaneous emission transition probabilities of Tm^{3+} : $^3F_4 \rightarrow {}^3H_6$ transition is $133.74s^{-1}$. The high spontaneous emission probabilities provide appropriate conditions for achieving great laser emission. Consequently, fluorotellurite glass is well suited to be the matrix material for 1.8 μm luminescence by Tm^{3+} : $^3F_4 \rightarrow {}^3H_6$ transition.

Table 1 Judd-Ofelt parameters Ω_t of Tm^{3+} in AYT3 glass

Glass	Ω_2	Ω_4	Ω_6	Reference
Fluoride	1.14	1.57	1.13	[35]
Tellurite	4.16	1.87	1.14	[15]
Silicate	3.17	0.56	0.58	[17]
AYT3	1.96	1.99	1.72	This work

Table 2 Calculated spontaneous transition probability (A_{rad}), total spontaneous transition probability ($\sum A$), branching ratios (β) and radiative lifetime (τ_{rad}) of AYT3 glass for various selected excited states of Tm^{3+}.

Transition	λ(nm)	$A_{rad}(s^{-1})$	$\sum A(s^{-1})$	β	τ_{rad} (ms)
$^3F_4 \rightarrow {}^3H_6$	1677	133.74	133.74	100.00%	7.48
$^3H_5 \rightarrow {}^3F_4$	1205	225.87	228.19	98.99%	4.38
$\rightarrow {}^3H_6$	3429	2.31		1.01%	
$^3H_4 \rightarrow {}^3H_6$	790	749.96	833.97	89.93%	1.20
$\rightarrow {}^3F_4$	1493	58.07		6.96%	
$\rightarrow {}^3H_6$	2293	25.94		3.11%	

3.5. Fluorescence spectral analysis

In order to investigate the relationship between the doping concentration of rare earth ions and the luminescence intensity, Fig.5(a) shows the fluorescence spectra of 1550-2150 nm of Tm^{3+} doped fluorotellurite glasses pumped by 808 nm laser diode. The central emission band at 1.8 μm corresponds to the energy level transition of Tm^{3+}: $^3F_4 \rightarrow {}^3H_6$. Inset of Fig.5(b) describes that the emission intensity increases and then decreases along with the increase of Tm^{3+} concentration. When Tm ion concentration is low, because of the large distance between Tm ions, energy transfer rate is not enough, leading to inefficient energy transfer. But as the concentration of the Tm ions increase, ions spacing becomes nearly until the ion concentration exceeds a certain value (3.5mol%), and the enhanced interaction leads to a great increment in the probability of energy transfer to the quenching center, which reduces the luminescence efficiency. It is obvious that AYT3 glass obtains the maximum emission intensity. In addition, we have obtained a broadband emission spectrum with large full-width at half-maximum (FWHM) which is usually used to evaluate the bandwidth characteristics of optical amplifiers. The relationship between the maximum FWHM of the 1.8um fluorescence and samples with different rare earth ion concentrations is shown in figure 5(b). With the increase of Tm^{3+} ion concentration, FWHM gradually widens and reaches a maximum of 216nm at AYT3. In the reported Tm^{3+} doped tellurite glass system, the half-height full width can only reach 160 nm[24] Compare with fluoroaluminate glass, the [TeO_3] units replace some [AlF_6] units in AYT3 glass, thus the Tm^{3+} distribution becomes more unsymmetrical, which indicates that the glass matrix has a wider range of bond lengths and angles. The divergences of the crystal filed split yield a range of electrostatic fields around Tm^{3+} ions in AYT3 glass. Therefore, an inhomogeneous broadening of the fluorescent band in present glass was achieved.

To further study the broadband characteristics of fluorotellurite glasses, effective half-width ($\Delta\lambda_{eff}$) are investigated using fluorescence spectra, we often use a more concise formula to describe the effective emission bandwidth as[36]:

$$\Delta\lambda_{eff}=\frac{\int I(\lambda)\, d\lambda}{I_{max}} \tag{2}$$

where $I(\lambda)$ is the fluorescence intensity at a wavelength of λ, and I_{max} is the maximum fluorescence intensity. The $\Delta\lambda_{eff}$ value is the largest at sample AYT3 (225.52 nm). The relatively large $\Delta\lambda_{eff}$ indicates AYT3 glass is an attractive candidate as gain medium in ultrashort pulse generation. As a consequence, the Tm^{3+} doped fluorotellurite glasses are potential matrix materials for application to optical fiber amplifiers.

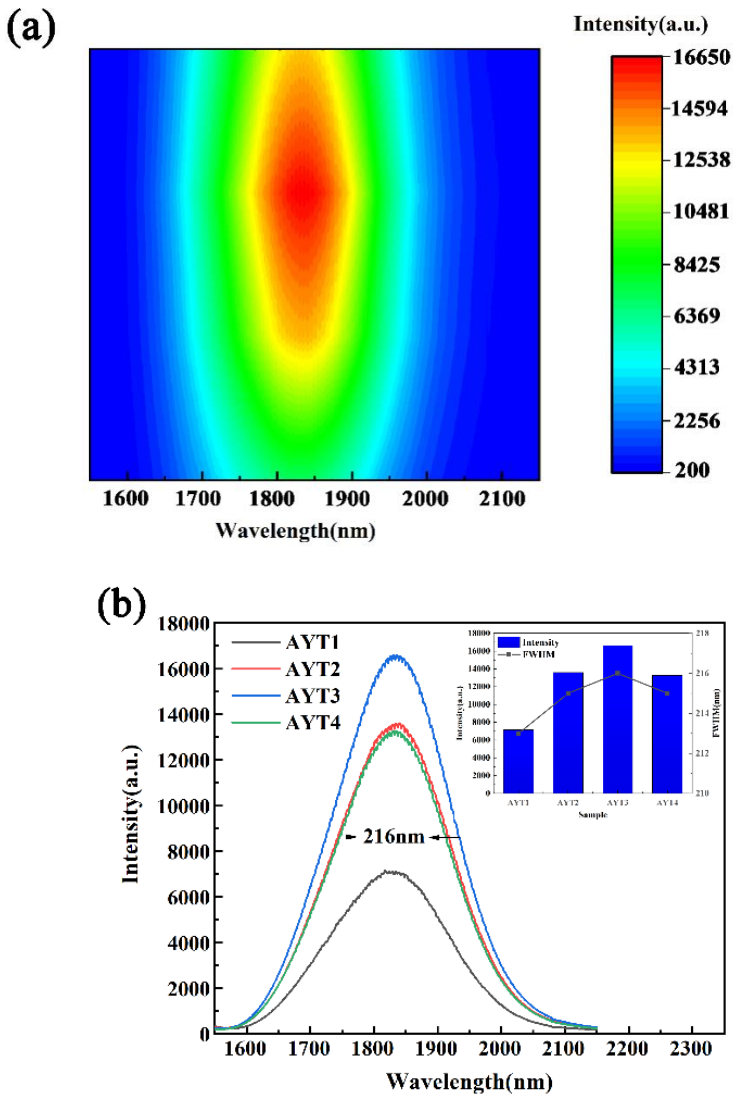

Fig.5(a) Emission spectra for Tm^{3+} doped AYT glasses in 1.8μm (b) Emission intensity for different concentrations and FWHM of AYT glasses

3.6. Lifetime and quantum efficiency and energy transfer

The fluorescence decay curves of AYT3 glass at 1800 nm are monitored and presented in Figure 6. It is obvious that the luminescence decay curve at Tm^{3+}: $^3F_4$ level of AYT3 glass is 5.68ms which is considerably larger than tellurite glass (1.83ms)[37] and smaller than fluoride glass(6.27ms)[18].

The quantum efficiency is an important parameter used to characterize the luminescence of laser glasses. In practical experiments, the quantum efficiency is related to the highest phonon energy of the substrate glass. The maximum phonon energy has the greatest effect on the non-radiative relaxation. Based on the spontaneous radiative lifetime (τ_{mea}) calculated from J-O parameters and the measured fluorescence lifetime (τ_{mea}), η can be calculated by following equation:

$$\eta = \frac{\tau_{mea}}{\tau_{rad}} \times 100\% \quad (3)$$

The quantum efficiency of Tm^{3+} fluorotellurite doped glass is 75.93%, which is much higher than that of Tm^{3+} doped tellurite glass (24%)[15]. Fluorotellurite glass with higher quantum efficiency is a potential material for 1.8 μm luminescence.

The insert of Figure 6, shows the simplified energy level diagram of $Tm^{3+}$and energy transfer processes to illustrate the 1.8 μm emission. When prepared Tm^{3+} doped glass pumped by 808 nm LD, the ground level of Tm^{3+} ($^3H_6$) are excited to the $^3H_4$ by ground state absorption (GSA:$^3H_6$+a photon (808 nm) →$^3H_4$)., then some Tm^{3+} ions on $^3H_4$ relax to the $^3F_4$ level, and cross-relaxation is generated with some other Tm^{3+} in the ground state $^3H_6$ energy level (CR: $^3H_4$+$^3H_6$→$^3F_4$+$^3F_4$) to the $^3F_4$ level. At the same time, the $^3H_4$ energy level in the higher energy state will transfer energy to the neighboring Tm^{3+} through energy transfer (ET: $^3H_4$→$^3H_4$) and then decay to the $^3F_4$ energy level. Therefore, a large number of ions in the sub-stable $^3F_4$ energy level will transit to the ground state and obtain 1.8 μm fluorescence emission.

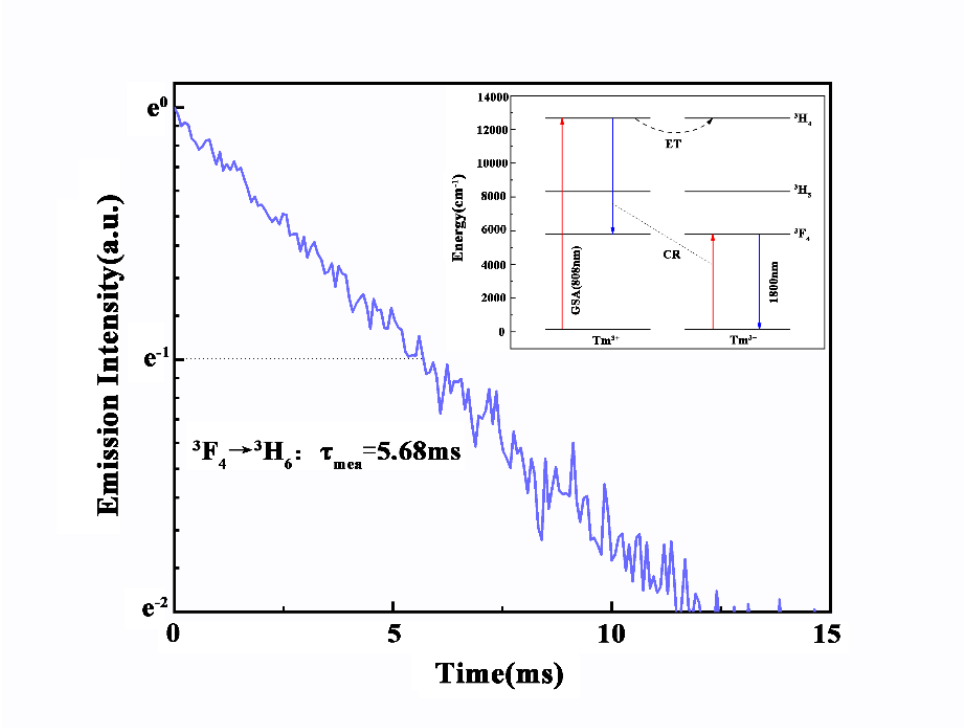

Fig.6 Fluorescence decay curves of the Tm^{3+}: $^3F_4$ level in AYT3 glass. Insert is simplified energy level diagram of Tm^{3+}

3.7 Absorption and emission cross sections

The absorption cross section and emission cross section are calculated in order to characterize the spectroscopic properties of the 1.8 μm emission. The absorption cross section ($\sigma_{abs}(\lambda)$) can be obtained from the absorption spectra using the Beer-Lambert law as follows[38]:

$$\sigma_{abs}(\lambda) = \frac{2.303lg(I_0/I)}{NI} \quad (4)$$

where $\lg(I_0/I)$ is the absorption intensity, N is the rare earth ion concentration, and l is the thickness of the prepared sample. The emission cross section can be calculated by the Füchtbauer-Ladenburg (FL) equation[39] from the absorption cross section:

$$\sigma_{emi}(\lambda) = \frac{\lambda^4 A_{rad}}{8\pi c n^2} \times \frac{\lambda I(\lambda)}{\int \lambda I(\lambda)\, d\lambda} \quad (5)$$

where A_{rad} is the spontaneous emission probability, λ corresponds wavelength, n is the refractive index, c is the speed of the light and $I(\lambda)$ is the emission intensity.

Figure 7 gives the absorption cross section and emission cross section of fluorotellurite glass. The maximum value of the absorption cross section for the Tm^{3+} ion at the $^3F_4 \rightarrow {}^3H_6$ is $2.54\times10^{-21}cm^2$ at 1675 nm and $4.11\times10^{-21}cm^2$ for the emission cross section at 1896nm. The larger emission cross section is beneficial for the laser effect. In addition, the FWHM$\times\sigma_{em}^{peak}$ is a reliable parameter to evaluate the gain medium. In this work, the calculated gain coefficient is $8.87\times10^{-26}cm^3$, which is larger than that of fluoride glass ($7.68\times10^{-26}cm^3$)[40]. The results show that the prepared fluorotellurite glass has good gain performance for 1.8 μm applications.

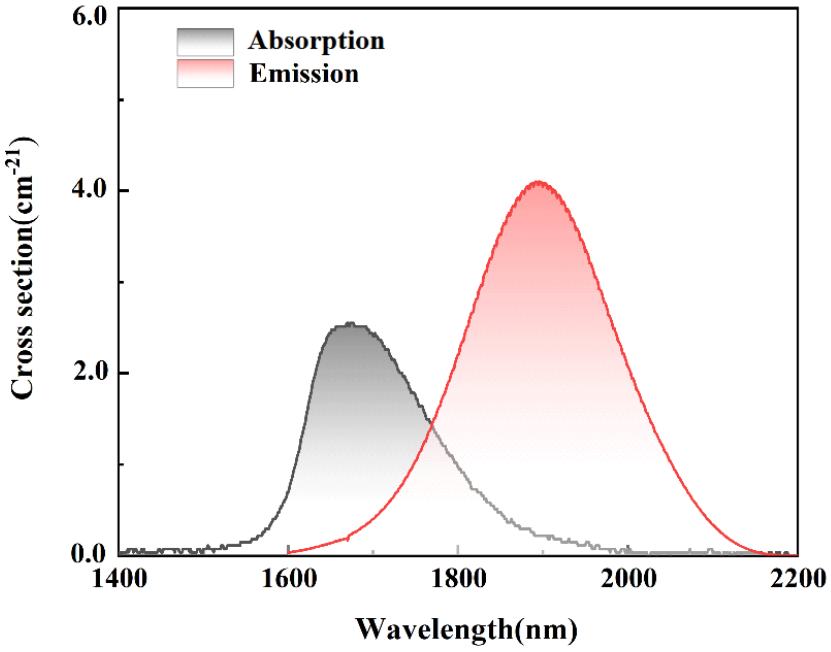

Fig.7 Calculated absorption and emission cross section of the AYT glass

4. Conclusions

In summary, Tm^{3+} doped fluorotellurite glass is prepared by high temperature melting method. The luminescence properties and thermal stability are studied. TeO_2 is introduced to overcome the defect of poor forming ability of fluoride glass. The transmittance of prepared fluorotellurite glass is as high as 91% . An effective 1.8 μm luminescence is obtained and FWHM reached 216nm. The emission cross section is calculated to be 4.11×10^{-21} cm^2 by using the measured emission spectra. The fluorescence lifetime of Tm^{3+} reaches 5.68ms, which is related to the lower phonon

energy(815cm^{-1}). Due to the cross-relaxation phenomenon of Tm^{3+}, the quantum efficiency achieved is 75.93%. The results show that Tm^{3+} doped fluorotellurite glass has potential application prospect in 1.8 μm laser materials.

Acknowledgement

The authors are thankful to National Key Research and Development Project of China(2018YFE0207700), the Zhejiang Provincial Natural Science Foundation of Chi na (LZ21F050002),the National Natural Science Foundation of China (nos.61775205).

Reference

[1] Walsh BM, Review of Tm and Ho materials; spectroscopy and lasers. Laser Physics 2009, 19(4):855-866.

[2] Taherunnisa S, Rudramamba KS, KrishnaReddy DV, Venkateswarlu T, Zhydachevskyy Y, Suchocki A, Piasecki M, RamiReddy M, Efficient 2.01 μm mid-infrared (MIR) and visible emission in Ho^{3+} doped phosphate glasses enhanced by Er^{3+} ions. Infrared Physics & Technology 2020, 107.

[3] Richards B, Jha A, Tsang Y, Binks D, Lousteau J, Fusari F, Lagatsky A, Brown C, Sibbett W, Tellurite glass lasers operating close to 2μm. Laser Physics Letters 2010, 7(3):177-193.

[4] Petersen CR, Lotz MB, Markos C, Woyessa G, Furniss D, Seddon AB, Taboryski RJ, Bang O, Thermo-mechanical dynamics of nanoimprinting anti-reflective structures onto small-core mid-IR chalcogenide fibers. Chinese Optics Letters 2021, 19(3):030603.

[5] Song X, Han K, Zhou D, Xu P, Zhang P, Broadband ~1.8 μm emission characteristics of Tm^{3+}-doped bismuth germanate glass based on Ga_2O_3 modification. Journal of Non-Crystalline Solids 2021, 557.

[6] Azam M, Rai VK, Ho^{3+} -Yb^{3+} codoped tellurite based glasses in visible lasers and optical devices: Judd-Ofelt analysis and frequency upconversion. Solid State Sciences 2017, 66:7-15.

[7] Shen D, Qian J, Wang C, Wang G, Wang X, Zhao Q, Facile preparation of silver nanoparticles in bulk silicate glass by high-repetition-rate picosecond laser pulses. Chinese Optics Letters 2021, 19(1):011901.

[8] Juárez-Hernández M, Mejía E, Spectral analysis of short-wavelength emission by up-conversion in a Tm^{3+}: ZBLAN dual-diode-pumped optical fiber. Chinese Optics Letters 2020, 18(7):071901.

[9] Sun Z, Wang F, Xia H, Nie H, Yang K, Wang R, He J, Zhang B, Spectroscopic and laser properties of Er^{3+}, Pr^{3+} co-doped $LiYF_4$ crystal. Chinese Optics Letters 2021, 19(8):081404.

[10] Kwiatkowski J, Power and spectral analyses in diode-pumped c-cut Pbnm Tm: YAP laser. Chinese Optics Letters 2020, 18(9):091401.

[11] Wang M, Liu M, Chen Y, Ouyang D, Zhao J, Pei J, Ruan S, Stable noise-like pulse generation in all-PM mode-locked Tm-doped fiber laser based on NOLM. Chinese Optics Letters 2021, 19(9):091402.

[12] Ji E, Shi J, Zha C, Zeng J, Zhou X, He Z, Yao Y, Lü Q, Ultimate capacity analysis of cladding-pumped 10/130 Tm: fiber laser. Chinese Optics Letters 2020, 18(5):051404.

[13] Xu R, Tian Y, Hu L, Zhang J, Broadband 2 μm emission and energy-transfer properties of thulium-doped oxyfluoride germanate glass fiber. Applied Physics B 2011, 104(4):839-844.

[14] Li J, Li C, Chen Y, Zhao N, Hou Z, Zhang Q, Zhou G, Broadband fluorescence emission in Bi-doped silica glass prepared by laser additive manufacturing technology. Chinese Optics Letters 2020, 18(12):121601.

[15] Lachheb R, Damak K, Assadi AA, Herrmann A, Yousef E, Rüssel C, Maâlej R, Characterization of Tm^{3+} doped TNZL glass laser material. Journal of Luminescence 2015, 161:281-287.

[16] Zhou D, Bai X, Zhou H, Preparation of Ho^{3+}/Tm^{3+} Co-doped Lanthanum Tungsten Germanium Tellurite Glass Fiber and Its Laser Performance for 2.0 μm. Sci Rep 2017, 7:44747.

[17] Liu X, Li M, Wang X, Huang F, Ma Y, Zhang J, Hu L, Chen D, ~2μm Luminescence properties and nonradiative processes of Tm^{3+} in silicate glass. Journal of Luminescence 2014, 150:40-45.

[18] Qi F, Huang F, Lei R, Tian Y, Zhang L, Zhang J, Xu S, Emission properties of 1.8 and 2.3 μm in Tm^{3+}-doped fluoride glass. Glass Physics and Chemistry 2017, 43(4):340-346.

[19] Xie J, Zhang Q, Zhuang Y, Liu X, Guan M, Zhu B, Yang R, Qiu J, Enhanced mid-IR emission in Yb^{3+}/Tm^{3+} co-doped oxyfluoride glass ceramics. Journal of Alloys and Compounds 2011, 509(6):3032-3037.

[20] Wang X, Fan S, Li K, Zhang L, Wang S, Hu L, Compositional dependence of the 1.8 μm emission properties of Tm^{3+} ions in silicate glass. Journal of Applied Physics 2012, 112(10).

[21] Ivanova S, Pellé F, Strong 1.53 μm to NIR–VIS–UV upconversion in Er-doped fluoride glass for high-efficiency solar cells. Optical Society of America 2009, 26(10):1930-1938.

[22] Huang F, Ma Y, Liu L, Hu L, Chen D, Enhanced 2.7μm emission of Er^{3+}-doped low hydroxyl fluoroaluminate–tellurite glass. Journal of Luminescence 2015, 158:81-85.

[23] Lebullenger R, Benjaballah S, Le Deit C, Poulain M, Systematic substitutions in ZBLA and ZBLAN glasses. Journal of non-crystalline solids 1993, 161:217-221.

[24] Zhou D, Wang R, Yang Z, Song Z, Yin Z, Qiu J, Spectroscopic properties of Tm^{3+} doped TeO_2-R_2O-La_2O_3 glasses for 1.47μm optical amplifiers. Journal of Non-Crystalline Solids 2011, 357(11-13):2409-2412.

[25] Peng YP, Yuan X, Zhang J, Zhang L, The effect of La_2O_3 in Tm^{3+}-doped germanate-tellurite glasses for ~2 μm emission. Sci Rep 2014, 4:5256.

[26] Klimesz B, Lisiecki R, Ryba-Romanowski W, Thermosensitive Tm^{3+}/Yb^{3+} co-doped oxyfluorotellurite glasses – spectroscopic and temperature sensor properties. Journal of Alloys and Compounds 2020, 823.

[27] Xu R, Tian Y, Hu L, Zhang J, Enhanced emission of 2.7 μm pumped by laser diode from Er^{3+}/Pr^{3+}-codoped germanate glasses. Optics Letters 2011, 36(7):1173-1175.

[28] Tian Y, Xu R, Hu L, Zhang J, 2.7μm fluorescence radiative dynamics and energy transfer between Er^{3+} and Tm^{3+} ions in fluoride glass under 800nm and 980nm excitation. Journal of Quantitative Spectroscopy and Radiative Transfer 2012, 113(1):87-95.

[29] Fares H, Jlassi I, Elhouichet H, Férid M, Investigations of thermal, structural and optical properties of tellurite glass with WO_3 adding. Journal of Non-Crystalline Solids 2014, 396-397:1-7.

[30] Wei T, Chen F, Tian Y, Xu S, Efficient 2.7μm emission and energy transfer mechanism in Er^{3+} doped Y_2O_3 and Nb_2O_5 modified germanate glasses. Journal of Quantitative Spectroscopy and Radiative Transfer 2014, 133:663-669.

[31] Li H, Lousteau J, MacPherson WN, Jiang X, Bookey HT, Barton JS, Jha A, Kar AK, Thermal sensitivity of tellurite and germanate optical fibers. OPTICS EXPRESS 2007, 15(14):8857-8863.

[32] Nazabal V, Todoroki S, Nukui A, Matsumoto T, Suehara S, Hondo T, Araki T, Inoue S, Rivero C, Cardinal T, Oxyfluoride tellurite glasses doped by erbium: thermal analysis, structural organization and spectral properties. Journal of Non-Crystalline Solids 2003, 325(1-3):85-102.

[33] Tang G, Zhu T, Liu W, Lin W, Qiao T, Sun M, Chen D, Qian Q, Yang Z, Tm^{3+} doped lead silicate glass single mode fibers for 2.0 μm laser applications. Optical Materials Express 2016, 6(6).

[34] Hehlen MP, Brik MG, Krämer KW, 50th anniversary of the Judd–Ofelt theory: An experimentalist's view of the formalism and its application. Journal of Luminescence 2013, 136:221-239.

[35] Bloembergen N, Encounters In Nonlinear Optics: Selected Papers of Nicolaas Bloembergen (With Commentary): World Scientific; 1996.

[36] Wei T, Tian C, Cai M, Tian Y, Jing X, Zhang J, Xu S, Broadband 2μm fluorescence and energy transfer evaluation in Ho^{3+}/Er^{3+} codoped germanosilicate glass. Journal of Quantitative Spectroscopy and Radiative Transfer 2015, 161:95-104.

[37] Li K, Zhang Q, Bai G, Fan S, Zhang J, Hu L, Energy transfer and 1.8μm emission in Tm^{3+}/Yb^{3+} codoped lanthanum tungsten tellurite glasses. Journal of Alloys and Compounds 2010, 504(2):573-578.

[38] Zhu T, Tang G, Chen X, Sun M, Qian Q, Chen D, Yang Z, Two micrometer fluorescence emission and energy transfer in Yb^{3+}/Ho^{3+}co-doped lead silicate glass. International Journal of Applied Glass Science 2016, 8(2):196-203.

[39] Lu Y, Cai M, Cao R, Tian Y, Huang F, Xu S, Zhang J, Enhanced effect of Er^{3+} ions on 2.0 and 2.85 μm emission of Ho^{3+} /Yb^{3+} doped germanate-tellurite glass. Optical Materials 2016, 60:252-257.

[40] Peng B, Izumitani TJOM, Optical properties, fluorescence mechanisms and energy transfer in Tm^{3+}, Ho^{3+} and Tm^{3+}-Ho^{3+} doped near-infrared laser glasses, sensitized by Yb^{3+}. Optical Materials 1995, 4(6):797-810.